GEOPHYSICS, VOL. 73, NO. 5 (SEPTEMBER-OCTOBER 2008); P. F197–F211, 13 FIGS., 4 TABLES.
10.1190/1.2973462

Generalized effective-medium theory of induced polarization

Michael Zhdanov[1]

ABSTRACT

A rigorous physical-mathematical model of heterogeneous conductive media is based on the effective-medium approach. A generalization of the classical effective-medium theory (EMT) consists of two major parts: (1) introduction of effective-conductivity models of heterogeneous, multiphase rock formations with inclusions of arbitrary shape and conductivity using the principles of the quasi-linear (QL) approximation within the framework of the EMT formalism and (2) development of the generalized effective-medium theory of induced polarization (GEMTIP), which takes into account electromagnetic-induction (EMI) and induced polarization (IP) effects related to the relaxation of polarized charges in rock formations. The new generalized EMT provides a unified mathematical model of heterogeneity, multiphase structure, and the polarizability of rocks. The geoelectric parameters of this model are determined by the intrinsic petrophysical and geometric characteristics of composite media: the mineralization and/or fluid content of rocks and the matrix composition, porosity, anisotropy, and polarizability of formations. The GEMTIP model allows one to find the effective conductivity of a medium with inclusions that have arbitrary shape and electrical properties. One fundamental IP model of an isotropic, multiphase, heterogeneous medium is filled with spherical inclusions. This model, because of its relative simplicity, makes it possible to explain the close relationships between the new GEMTIP conductivity-relaxation model and an empirical Cole-Cole model or classical Wait's model of the IP effect.

INTRODUCTION

The electromagnetic (EM) data observed in geophysical experiments generally reflect two phenomena: (1) electromagnetic induction (EMI) in the earth and (2) the induced polarization (IP) effect related to the relaxation of polarized charges in rock formations. The theoretical and experimental foundations of induced polarization (IP) methods in geophysical exploration were developed by several generations of geophysicists, starting with the pioneering research of the Schlumberger brothers and continued by A. S. Semenov, Y. P. Bulashevich, S. M. Sheinman, V. A. Komarov, T. Madden, H. Seigel, J. Wait, S. Ward, J. Hohmann, K. Zonge, and many others (see review by Seigel et al., 2007).

Practical use of the IP method can be traced to the 1950s, when mining and petroleum companies actively looked into application of this method to mineral exploration. The physical-mathematical principles of the IP effect originally were formulated in pioneering works by Wait (1959) and by Sheinman (1969). However, this method did not find wide application in U. S. industry until after the work of Zonge and his associates at the Zonge Engineering and Research Organization (Zonge, 1974; Zonge and Wynn, 1975) and by Pelton (1977) and Pelton et al. (1978) at the University of Utah. Significant contribution to the development of the IP method was made also by Wait (1959, 1982) and by the research team at Kennecott from 1965 through 1977 (Nelson, 1997).

The IP method has found wide application in mining exploration. Interpretation of IP data in the mining industry was improved significantly during the last decade based on the advanced interpretation techniques developed by Oldenburg and coauthors (e.g., Oldenburg and Li, 1994; Yuval and Oldenburg, 1997). There was also an interesting proposed application of the IP method to well logging (e.g., Vinegar and Waxman, 1988), and Russian geophysicists reported successful applications of the IP method in hydrocarbon exploration (e.g., Komarov, 1980; Zonge, 1983; Kamenetsky, 1997; Davydycheva et al., 2004).

The IP effect is caused by the complex EM phenomena that accompany current flow in the earth. These phenomena occur in rock formations in areas of mineralization. It was demonstrated almost 30 years ago in pioneering papers by Zonge and Wynn (1975) and by Pelton et al. (1978) that the IP effect can be used to separate the responses of economic polarizable targets from other anomalies. However, until recently, this idea had a limited practical application because of the difficulties in recovering the induced polarization parameters from observed EM data, especially in the 3D interpretation required for efficient exploration of mining and petroleum targets

Manuscript received by the Editor 29 October 2007; revised manuscript received 25 April 2008; published online 17 September 2008.
[1]University of Utah, Department of Geology and Geophysics, Salt Lake City, Utah, U.S.A. E-mail: mzhdanov@mines.utah.edu.

and because of the absence of adequate composite-conductivity models of rock formations.

The analysis of IP phenomena usually is based on models with frequency-dependent complex conductivity distribution. One of the most popular is the Cole-Cole relaxation model and its different modifications (Cole and Cole, 1941). The parameters of the conductivity-relaxation model can be used for discrimination of different types of rock formations, an important goal in mineral exploration. Until recently, these parameters have been determined mostly in the physical laboratory by direct analysis of samples.

I introduce a new composite geoelectric model of rock formations based on the effective-medium approach that generates a conductivity model with parameters directly related by analytic expressions to the physical characteristics of the microstructure of rocks and minerals (microgeometry and conductivity parameters). This new composite geoelectric model provides more realistic representation of complex rock formations than conventional unimodal-conductivity models. It allows us to model the relationships between the geometric factors and physical characteristics of different types of rocks (e.g., grain size, shape, conductivity, polarizability, fraction volume, and so forth) and the parameters of the relaxation model.

Effective-medium approximation for composite media has been discussed in many publications. The general formalism of the effective-medium theory (EMT) was developed by Stroud (1975). The advances of physical EMTs (e.g., Landauer, 1978; Norris et al., 1985; Shwartz, 1994; Sihvola, 2000; Kolundzija and Djordjevic, 2002; Berryman, 2006) make it possible to develop a rigorous mathematical model of multiphase heterogeneous conductive media excited by an EM field. The EMT and its different extensions were applied successfully to the study of macroscopically isotropic and anisotropic models of rock formations in electrical geophysics (e.g., Mendelson and Cohen, 1982; Sen et al., 1981; Sheng, 1991; Kazatchenko et al., 2004; Toumelin and Torres-Verdín, 2007, and so forth).

The existing form of EMT and its modifications, however, do not allow the inclusion of the induced-polarizability effect in the general model of heterogeneous rocks. The conventional EMT models describe the electromagnetic-induction effect caused by electrical heterogeneity of the multiphase medium, whereas the IP effect is manifested by additional surface polarization of the grains caused by the complex electrochemical reactions that accompany current flow within the formation.

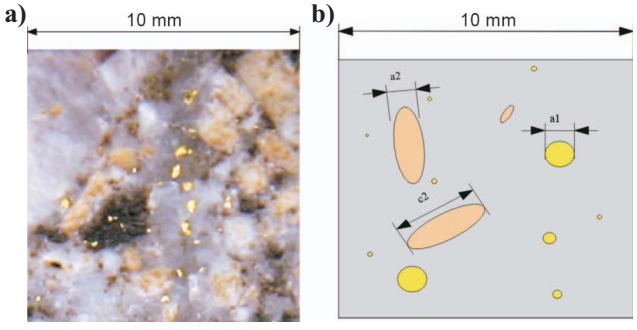

Figure 1. Multiphase composite model of general heterogeneous rocks. (a) A typical slice of a quartz monzonite porphyry (QMP) rock sample. (b) A schematic multiphase composite model of the same rock sample with the grains represented by spherical and elliptical inclusions.

It is well known, however, that the effective conductivity of rocks is not necessarily a constant and real number but can vary with frequency and be complex (Shuev and Johnson, 1973). There are several explanations for these properties of effective conductivity. Most often, they are explained by physical-chemical polarization effects of mineralized particles of rock material and/or by electrokinetic effects in the pores of reservoirs (Wait, 1959; Marshall and Madden, 1959; Luo and Zhang, 1998). Thus, polarizability is caused by the complex electrochemical reactions that accompany current flow in the earth. These reactions occur in a heterogeneous medium representing rock formations in areas of mineralization and hydrocarbon reservoirs. This phenomenon usually is explained as a surface polarization of mineralized particles and the surface of a moisture-porous space that occurs under the influence of an external electromagnetic field. It is manifested by accumulating electric charges on the surface of different grains forming the rock. This effect is very significant in the case of a metal-electrolyte interface (Bockrih and Reddy, 1973). However, a similar effect is observed in the interface between electrolyte and typical rock-forming minerals such as silicate and carbonate (Komarov, 1980).

I demonstrate that EMT formalism can be used in the theory of formation polarizability as well. A generalization of the classical EMT approach consists of two major parts: (1) introduction of the effective-conductivity models of the heterogeneous, multiphase rock formations with inclusions of arbitrary shape and conductivity by using the principles of the Born-type quasi-linear (QL) approximation in the framework of EMT formalism, and (2) development of the generalized effective-medium theory of induced polarization (GEMTIP), which takes into account electromagnetic induction (EMI) and induced polarization (IP) effects related to the relaxation of polarized charges in rock formations.

This paper details this generalized approach by treating EMI and IP effects in a complex rock formation in a unified way. I provide more information on the evolution of this method in Appendix A. The Born-type approximation in the framework of EMT theory was used recently by Habashy and Abubakar (2007) to derive a material-averaging formulation and to develop effective numerical methods for constructing finite-difference modeling grids to study rock heterogeneity.

The general model applies to mineralization zones and hydrocarbon reservoirs. It develops a unified physical-mathematical model to examine EM effects in complex rock formations that accounts for mineral structure, electrical properties, fluid content, matrix composition, porosity, anisotropy, and polarizability. It provides a link between the volume content of different minerals and/or the hydrocarbon saturations and the observed EM field data (Zhdanov, 2006a, 2006b, 2008).

PRINCIPLES OF THE EFFECTIVE-MEDIUM APPROACH

The goal is to construct realistic electrical models of rocks based on the EMT of multiphase composite media. We begin our modeling with an example taken from a typical quartz monzonite porphyry (QMP). Figure 1a presents a typical slice of a QMP rock sample containing grains of different minerals: quartz, feldspar, pyrite, chalcopyrite, and biotite. Figure 1b is a schematic multiphase composite model of the same rock sample with grains represented by spherical and elliptical inclusions of different sizes and orientations.

Note that in principle, one can consider a schematic multiphase model of a reservoir rock sample also (Figure 2a).

Figure 1 and the left panel of Figure 2 show that we can represent a complex heterogeneous rock formation as a composite model formed by a homogeneous host medium of a volume V with a (complex) conductivity tensor $\hat{\boldsymbol{\sigma}}_0(\mathbf{r})$ (where $\mathbf{r}$ is an observation point) filled with grains of arbitrary shape and conductivity. In the present problem, the rock is composed of a set of N different types of grains, the lth grain type having a (complex) tensor conductivity $\hat{\boldsymbol{\sigma}}_l$. The grains of the lth type have a volume fraction f_l in the medium and a particular shape and orientation. Therefore, the total conductivity tensor of the model, $\hat{\sigma}(\mathbf{r})$, has the following distribution for volume fraction f_l and volume fraction $f_0 = (1 - \Sigma_{l=1}^{N} f_l)$, respectively:

$$\hat{\boldsymbol{\sigma}}(\mathbf{r}) = \begin{cases} \hat{\boldsymbol{\sigma}}_0 \text{ for volume fraction } f_0 = \left(1 - \sum_{l=1}^{N} f_l\right) \\ \hat{\boldsymbol{\sigma}}_l \text{ for volume fraction } f_l. \end{cases}$$

For convenience, I present in Table 1 a list of variables used in this paper.

The polarizability effect usually is associated with surface polarization of the coatings of grains. This surface polarization can be related to an electrochemical charge transfer between the grains and a host medium (Wong, 1979; Wong and Strangway, 1981; Klein et al., 1984). The surface polarization is manifested by accumulating electric charges on the surface of the grain. A double layer of charges is created on the grain's surface, which results in a voltage drop at this surface (Wait, 1982). It has been shown experimentally that for relatively small external electric fields used in electrical exploration, the voltage drop, Δu, is linear and proportional to the normal current flow at the surface of the particle, $j_n = (\mathbf{n}\cdot\mathbf{j})$. That is, at the surface of the grain, we have

$$\Delta u = k(\mathbf{n}\cdot\mathbf{j}), \tag{1}$$

where $\mathbf{n}$ is a unit vector of the outer normal to the grain's surface and k is a surface-polarizability factor, which generally is a complex frequency-dependent function. This function usually is treated as the interface impedance that characterizes the boundary between the corresponding grain and surrounding host medium and describes the interfacial or membrane polarization. This effect is the most profound in a metal-electrolyte interface, and it was studied intensively in electrochemistry (Bockrih and Reddy, 1973). However, a similar effect also was found in other heterogeneous systems typical of rock formations (e.g., Dukhin, 1971).

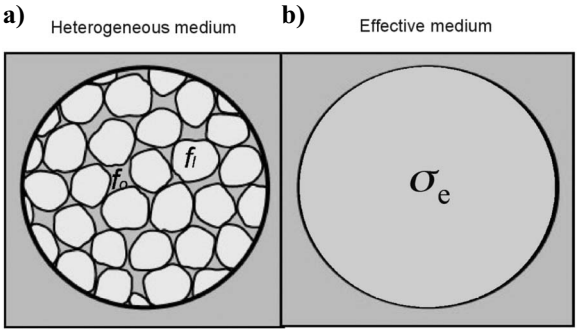

Figure 2. (a) A schematic multiphase heterogeneous model of a reservoir rock sample. (b) A corresponding effective-medium model.

Following the standard logic of the EMT, we substitute a homogeneous effective medium with the conductivity tensor $\hat{\sigma}_e$ for the original heterogeneous composite model (Figure 2) and subject it to a constant electric field, $\mathbf{E}^b$, equal to the average electric field in the original model:

$$\mathbf{E}^b = \langle\mathbf{E}\rangle = V^{-1}\int\int\int_V \mathbf{E}(\mathbf{r})dv. \tag{2}$$

The effective conductivity is defined by the current density distribution, $\mathbf{j}_e$, in an effective medium being equal to the average current density distribution in the original model:

$$\mathbf{j}_e = \hat{\boldsymbol{\sigma}}_e\cdot\mathbf{E}^b = \hat{\boldsymbol{\sigma}}_e\cdot\langle\mathbf{E}\rangle = \langle\hat{\boldsymbol{\sigma}}\cdot\mathbf{E}\rangle. \tag{3}$$

To find the effective conductivity tensor, $\hat{\sigma}_e$, we represent the given inhomogeneous composite model as a superposition of a homo-

Table 1. List of variables.

$\hat{\sigma}$	Total conductivity tensor
f_l	Volume fraction of a grain of the lth type
$\hat{\sigma}_0$	Conductivity tensor of a host medium
$\hat{\sigma}_l$	Conductivity tensor of a grain of the lth type
$\hat{\sigma}_e$	Conductivity tensor of a homogeneous effective medium
$\hat{\sigma}_b$	Conductivity tensor of a homogeneous background medium
$\Delta\hat{\sigma}$	Anomalous-conductivity tensor
Δu	Voltage drop at the grain's surface
k	Surface-polarizability factor
$\mathbf{E}^b$	Average electric field in the original model
$\hat{\hat{\mathbf{e}}}$	Electrical-reflectivity tensor
$\hat{\mathbf{m}}$	Material-property tensor
$\hat{\mathbf{G}}_b$	Green's tensor for the homogeneous background full space
$\hat{\boldsymbol{\Gamma}} = \int\int\int_V \hat{\mathbf{G}}_b dv$	Volume-depolarization tensor
$\hat{\boldsymbol{\Lambda}} = \int\int_S \hat{\mathbf{G}}_b\cdot\mathbf{nn}ds$	Surface-depolarization tensor
$\hat{\xi} = k\sigma_b\hat{\sigma}\cdot(\Delta\hat{\sigma})^{-1}$	Relative-conductivity tensor
$\hat{\mathbf{p}} = \hat{\boldsymbol{\Gamma}}^{-1}\cdot\hat{\boldsymbol{\Lambda}}\cdot\hat{\xi}$	Surface-polarizability tensor
$\hat{\mathbf{q}} = [\hat{\mathbf{I}} + \hat{\mathbf{p}}]\cdot\hat{\mathbf{m}}$	Volume-polarizability tensor
$\Delta\hat{\sigma}^p = [\hat{\mathbf{I}} + \hat{\mathbf{p}}]\cdot\Delta\hat{\sigma}$	"Polarized" anomalous conductivity
ρ_0	DC resistivity of the Cole-Cole model
ω	Angular frequency
τ and C	Time and relaxation parameters of the Cole-Cole model
η	Chargeability coefficient
α	Surface-polarizability coefficient
a	Radius of a spherical grain

geneous infinite background medium with the conductivity tensor $\hat{\sigma}_b$ and the anomalous conductivity $\Delta\hat{\sigma}(\mathbf{r})$:

$$\hat{\boldsymbol{\sigma}}(\mathbf{r}) = \hat{\boldsymbol{\sigma}}_b + \Delta\hat{\boldsymbol{\sigma}}(\mathbf{r}). \quad (4)$$

Note that this representation is not unique. Different methods exist for selecting the appropriate background conductivity $\hat{\sigma}_b$. Some of these methods will be discussed below.

From equations 4 and 3, we have

$$\hat{\boldsymbol{\sigma}}_e \cdot \mathbf{E}^b = \hat{\boldsymbol{\sigma}}_b \cdot \mathbf{E}^b + \langle \Delta\hat{\boldsymbol{\sigma}} \cdot \mathbf{E} \rangle. \quad (5)$$

Thus we can see that the effective conductivity tensor, $\hat{\sigma}_e$, can be found from equation 5 if one determines the average excess electric current $\langle \Delta\hat{\sigma} \cdot \mathbf{E} \rangle$. The last problem can be solved using the integral form of Maxwell's equations.

Following the ideas of the QL approximation (Zhdanov, 2002), we can represent the electric field as

$$\mathbf{E}(\mathbf{r}') = (\hat{\mathbf{I}} + \hat{\boldsymbol{\lambda}}(\mathbf{r}')) \cdot \mathbf{E}^b, \quad (6)$$

where $\hat{\boldsymbol{\lambda}}(\mathbf{r}')$ is an electrical reflectivity tensor, and

$$\Delta\hat{\boldsymbol{\sigma}}(\mathbf{r}') \cdot \mathbf{E}(\mathbf{r}') = \hat{\mathbf{m}}(\mathbf{r}') \cdot \mathbf{E}^b, \quad (7)$$

where $\hat{\mathbf{m}}(\mathbf{r}')$ is a material property tensor (similar to the susceptibility tensor in the theory of EM field propagation in dielectrics):

$$\hat{\mathbf{m}}(\mathbf{r}') = \Delta\hat{\boldsymbol{\sigma}}(\mathbf{r}') \cdot (\hat{\mathbf{I}} + \hat{\boldsymbol{\lambda}}(\mathbf{r}')). \quad (8)$$

Note that one can use the extended Born approximation, another form of the Born-type approximations, to obtain an expression similar to equation 6 (e.g., see Abubakar and Habashy, 2005). However, I prefer to use the QL formulation in this case because it can generate an approximate or even a rigorous solution depending on the appropriate choice of the reflectivity tensor $\hat{\boldsymbol{\lambda}}$. It is important to emphasize that exact representations 6 and 7 always exist because the corresponding material property tensor always can be found for any fields $\mathbf{E}(\mathbf{r}')$ and $\mathbf{E}^b$ (Zhdanov, 2002). In this paper, I explicitly use this special case, when the QL "approximation" is not an approximation but an exact form of the field representation. I should note also that Habashy and Abubakar (2007) have employed this idea of using the Born-type approximation within the framework of the EMT theory for development of a material-averaging formula based on the extended Born approximation. They have demonstrated that this approach can provide an effective numerical method for constructing the finite-difference modeling grids to study rock heterogeneity.

Let us substitute equation 7 into equation 3, taking into account equation 4,

$$\mathbf{j}_e = \hat{\boldsymbol{\sigma}}_e \cdot \mathbf{E}^b = \langle \hat{\boldsymbol{\sigma}} \cdot \mathbf{E} \rangle = \langle (\hat{\boldsymbol{\sigma}}_b + \Delta\hat{\boldsymbol{\sigma}}) \cdot \mathbf{E} \rangle = \hat{\boldsymbol{\sigma}}_b \cdot \langle \mathbf{E} \rangle + \langle \Delta\hat{\boldsymbol{\sigma}} \cdot \mathbf{E} \rangle = \hat{\boldsymbol{\sigma}}_b \cdot \mathbf{E}^b + \langle \hat{\mathbf{m}} \rangle \cdot \mathbf{E}^b.$$

From the last equation, we see that

$$\hat{\boldsymbol{\sigma}}_e = \hat{\boldsymbol{\sigma}}_b + \langle \hat{\mathbf{m}} \rangle. \quad (9)$$

Thus, to determine the effective conductivity of the composite polarized medium, we have to find the average value of the material property tensor, $\langle \hat{\mathbf{m}} \rangle$.

INTEGRAL REPRESENTATIONS FOR THE EM FIELD IN HETEROGENOUS POLARIZABLE MEDIA

One can represent the electric field $\mathbf{E}(\mathbf{r})$ generated in a homogeneous anisotropic background medium by the currents induced within the anomalous conductivity $\Delta\hat{\sigma}(\mathbf{r})$ using the integral form of Maxwell's equations,

$$\mathbf{E}(\mathbf{r}) = \mathbf{E}^b + \int\int\int_V \hat{\mathbf{G}}_b(\mathbf{r}/\mathbf{r}') \cdot [\Delta\hat{\boldsymbol{\sigma}}(\mathbf{r}') \cdot \mathbf{E}(\mathbf{r}')] dv', \quad (10)$$

where V is the volume occupied by all inhomogeneities and $\hat{\mathbf{G}}_b(\mathbf{r}/\mathbf{r}')$ is a Green's tensor for the homogeneous, anisotropic full space.

To simplify further discussion, we assume that the background model is represented by the isotropic homogeneous full space $\hat{\sigma}_b = \hat{\mathbf{I}}\sigma_b$. We also restrict our discussion of the generalized EMT to the quasi-static case, when $a_l/w_l \ll 1$; a_l is the characteristic size of a grain of the lth type, and w_l is a wavelength in that grain. This restriction means we do not consider high frequencies or high contrasts of electrical resistivity in our model to simplify further derivations. In this case, the Green's tensor can be represented in the form of a dyadic function,

$$\hat{\mathbf{G}}_b(\mathbf{r}/\mathbf{r}') = \nabla\nabla' g_b(\mathbf{r}/\mathbf{r}'), \quad (11)$$

where

$$g_b(\mathbf{r}/\mathbf{r}') = \frac{1}{4\pi\sigma_b|\mathbf{r} - \mathbf{r}'|}. \quad (12)$$

We assume, however, that in addition to electrical heterogeneity, the medium is characterized by polarizability effects that are manifested by the surface polarization of the grains. Mathematically, the surface-polarization effect can be included in the general system of Maxwell's equations by adding the following boundary conditions on the surfaces S_l of the grains (Luo and Zhang, 1998):

$$[\mathbf{n} \times (\mathbf{E}^+(\mathbf{r}') - E^-(\mathbf{r}'))]_{S_l} = -[\mathbf{n} \times \nabla'\Delta u(\mathbf{r}')]_{S_l}, \quad (13)$$

where $\mathbf{E}^+$ designates the boundary value of electric field $\mathbf{E}(\mathbf{r})$ when the observation point tends to the boundary S_l of the lth grain from the inside of the grains and $\mathbf{E}^-$ if this point tends to the boundary from the outside of the grains.

Therefore, an electric field caused by the surface-polarization effect $\mathbf{E}^p(\mathbf{r})$ can be represented as an electric field of a specified discontinuity 13 (Zhdanov, 1988):

$$\mathbf{E}^p(\mathbf{r}) = -\nabla \times \int\int_S g_b(\mathbf{r}/\mathbf{r}')\sigma_b \times [\mathbf{n}(\mathbf{r}') \cdot (\mathbf{E}^+(\mathbf{r}') - E^-(\mathbf{r}'))]_S \, ds', \quad (14)$$

where S represents the superposition of all surfaces S_l of the entire ensemble of grains, $S = \cup_{l=1}^{N} S_l$, and vector $\mathbf{n}(\mathbf{r}')$ is directed outside the grains.

The last integral can be written in an equivalent form as a field generated by the double layers coinciding with the grains' surfaces with a dipole electric-charge moment density $\mathbf{M}_S = \Delta u\mathbf{n}$ (Zhdanov, 1988):

$$\mathbf{E}^p(\mathbf{r}) = \nabla \int\int_S \nabla' g_b(\mathbf{r}/\mathbf{r}')\sigma_b \cdot \mathbf{n}(\mathbf{r}')\Delta u ds'. \quad (15)$$

According to equation 1, we assume that the voltage drop at the surface of the grain is proportional to the normal current:

$$\Delta u = k(\mathbf{n}(\mathbf{r}') \cdot \mathbf{j}(\mathbf{r}')) = k(\mathbf{n}(\mathbf{r}') \cdot \hat{\boldsymbol{\sigma}}(\mathbf{r}') \cdot \mathbf{E}(\mathbf{r}')), \quad (16)$$

where current $\mathbf{j}(\mathbf{r}')$ is taken for the internal side of the grain's surface.

Therefore, expression 14 becomes

$$\mathbf{E}^p(\mathbf{r}) = \nabla \int\int_S \nabla' g_b(\mathbf{r}/\mathbf{r}')\sigma_b \cdot \mathbf{n}(\mathbf{r}')\Delta u ds' = \int\int_S \hat{\mathbf{G}}_b(\mathbf{r}/\mathbf{r}') \cdot \mathbf{n}(\mathbf{r}')k\sigma_b(\mathbf{n}(\mathbf{r}') \cdot \hat{\sigma}(\mathbf{r}') \cdot \mathbf{E}(\mathbf{r}'))ds'. \quad (17)$$

The total electric field caused by the effects of both the electromagnetic induction and induced polarization is equal to

$$\mathbf{E}(\mathbf{r}) = \mathbf{E}^b + \int\int\int_V \hat{\mathbf{G}}_b(\mathbf{r}/\mathbf{r}') \cdot [\Delta\hat{\sigma}(\mathbf{r}') \cdot \mathbf{E}(\mathbf{r}')]dv' + \int\int_S \hat{\mathbf{G}}_b(\mathbf{r}/\mathbf{r}') \cdot \mathbf{n}(\mathbf{r}')k\sigma_b(\mathbf{n}(\mathbf{r}') \cdot \hat{\sigma}(\mathbf{r}') \cdot \mathbf{E}(\mathbf{r}'))ds'. \quad (18)$$

Substituting expression 7 into equation 18, we can write

$$\mathbf{E}(\mathbf{r}) = \mathbf{E}^b + \int\int\int_V \hat{\mathbf{G}}_b(\mathbf{r}/\mathbf{r}') \cdot [\hat{\mathbf{m}}(\mathbf{r}') \cdot \mathbf{E}^b]dv' + \int\int_S \hat{\mathbf{G}}_b(\mathbf{r}/\mathbf{r}') \cdot \mathbf{n}(\mathbf{r}') \times (\mathbf{n}(\mathbf{r}') \cdot \hat{\xi}(\mathbf{r}') \cdot [\hat{\mathbf{m}}(\mathbf{r}') \cdot \mathbf{E}^b])ds', \quad (19)$$

where $\hat{\xi}(\mathbf{r}')$ is the relative conductivity tensor of a grain equal to

$$\hat{\xi}(\mathbf{r}') = k\sigma_b\hat{\sigma}(\mathbf{r}') \cdot (\Delta\hat{\sigma}(\mathbf{r}'))^{-1}. \quad (20)$$

We can represent the integrals in equation 19 as a sum of the integrals over the volumes and surfaces of all grains:

$$\mathbf{E}(\mathbf{r}) = \mathbf{E}^b + \sum_l \mathbf{E}_l(\mathbf{r}), \quad (21)$$

where

$$\mathbf{E}_l(\mathbf{r}) = \int\int\int_{V_l} \hat{\mathbf{G}}_b(\mathbf{r}/\mathbf{r}') \cdot [\hat{\mathbf{m}}(\mathbf{r}') \cdot \mathbf{E}^b]dv' + \int\int_{S_l} \hat{\mathbf{G}}_b(\mathbf{r}/\mathbf{r}') \cdot \mathbf{n}(\mathbf{r}') \times (\mathbf{n}(\mathbf{r}') \cdot \hat{\xi}(\mathbf{r}') \cdot [\hat{\mathbf{m}}(\mathbf{r}') \cdot \mathbf{E}^b])ds'. \quad (22)$$

We already have noted that we will restrict our discussion to the low-frequency approximation (quasi-static model of the field). In this case, we can use a QL approximation (Zhdanov, 2002) for the integrals over V_l and S_l and assume that the material property tensor is constant in V_l up to its boundary S_l:

$$\hat{\mathbf{m}}(\mathbf{r}') = \hat{\mathbf{m}}_l, \mathbf{r}' \in V_l. \quad (23)$$

Note, however, that in the case of spherical or elliptical grains, the material property tensor is always constant within the spherical and/or elliptical inclusions. The rigorous proof of this simple property of the material property tensor comes from an analytic expression for the electric field of the elliptical inclusions in the homogeneous background, which can be found, for example, in Landau and Lifshitz (1984).

Consider now the integrals over one grain only:

$$\mathbf{E}_l(\mathbf{r}) = \int\int\int_{V_l} \hat{\mathbf{G}}_b(\mathbf{r}/\mathbf{r}')dv' \cdot \hat{\mathbf{m}}_l \cdot \mathbf{E}^b + \int\int_{S_l} \hat{\mathbf{G}}_b(\mathbf{r}/\mathbf{r}') \cdot \mathbf{n}(\mathbf{r}')\mathbf{n}(\mathbf{r}')ds' \cdot \hat{\xi}_l \cdot \hat{\mathbf{m}}_l \cdot \mathbf{E}^b, \quad (24)$$

where

$$\hat{\xi}(\mathbf{r}') = \hat{\xi}_l = const, \quad \mathbf{r}' \in V_l.$$

We introduce the volume, $\hat{\boldsymbol{\Gamma}}_l$, and surface, $\hat{\boldsymbol{\Lambda}}_l$, depolarization tensors as follows:

$$\hat{\boldsymbol{\Gamma}}_l = \int\int\int_{V_l} \hat{\mathbf{G}}_b(\mathbf{r}/\mathbf{r}')dv', \quad (25)$$

and

$$\hat{\boldsymbol{\Lambda}}_l = \int\int_{S_l} \hat{\mathbf{G}}_b(\mathbf{r} \cdot \mathbf{r}') \cdot \mathbf{n}(\mathbf{r}')\mathbf{n}(\mathbf{r}')ds'. \quad (26)$$

In the case of spherical or elliptical grains, one can derive the exact analytic expressions for the depolarization tensors. In this paper, as an illustration, we will consider spherical grains only. A similar result for elliptical grains is presented in Zhdanov et al. (2008), in which the authors study the anisotropy in the IP effect.

For example, for a spherical grain of a radius a_l, we have (see Appendix B)

$$\hat{\boldsymbol{\Gamma}}_l = -\frac{1}{3\sigma_b}\hat{\mathbf{I}}, \quad \hat{\boldsymbol{\Lambda}}_l = -\frac{2}{3\sigma_b a_l}\hat{\mathbf{I}}. \quad (27)$$

Substituting equations 25 and 26 back into equation 24, we obtain

$$\mathbf{E}_l(\mathbf{r}) = \hat{\boldsymbol{\Gamma}}_l \cdot \hat{\mathbf{m}}_l \cdot \mathbf{E}^b + \hat{\boldsymbol{\Gamma}}_l \cdot \hat{\mathbf{p}}_l \cdot \hat{\mathbf{m}}_l \cdot \mathbf{E}^b = \hat{\boldsymbol{\Gamma}}_l \cdot \hat{\mathbf{q}}_l \cdot \mathbf{E}^b, \quad (28)$$

where a surface-polarizability tensor $\hat{\mathbf{p}}$ and a volume-polarizability tensor $\hat{\mathbf{q}}$ are equal to

$$\hat{\mathbf{p}}(\mathbf{r}') = \hat{\boldsymbol{\Gamma}}_l^{-1} \cdot \hat{\boldsymbol{\Lambda}}_l \cdot \hat{\xi}(\mathbf{r}'), \quad \hat{\mathbf{p}}_l = \hat{\mathbf{p}}(\mathbf{r}'), \mathbf{r}' \in V_l, \quad (29)$$

and

$$\hat{\mathbf{q}}(\mathbf{r}') = [\hat{\mathbf{I}} + \hat{\mathbf{p}}(\mathbf{r}')] \cdot \hat{\mathbf{m}}(\mathbf{r}'), \quad \hat{\mathbf{q}}_l = \hat{\mathbf{q}}(\mathbf{r}'), \ \mathbf{r}' \in V_l. \quad (30)$$

Then equation 28 becomes

$$\mathbf{E}_l(\mathbf{r}) = \int\int\int_{V_l} \hat{\mathbf{G}}_b(\mathbf{r}/\mathbf{r}')dv' \cdot \hat{\mathbf{q}}_l \cdot \mathbf{E}^b. \quad (31)$$

Substituting expression 31 back into expression 21, we find

$$\mathbf{E}(\mathbf{r}) = \mathbf{E}^b + \sum_l \int\int\int_{V_l} \hat{\mathbf{G}}_b(\mathbf{r}/\mathbf{r}') \cdot \hat{\mathbf{q}}(\mathbf{r}')dv' \cdot \mathbf{E}^b = \mathbf{E}^b + \int\int\int_V \hat{\mathbf{G}}_b(\mathbf{r}/\mathbf{r}') \cdot \hat{\mathbf{q}}(\mathbf{r}')dv' \cdot \mathbf{E}^b. \quad (32)$$

The last equation shows that the surface-polarization effect introduced by equation 17 can be represented by the equivalent volume-polarization effect and combined with the electromagnetic-induction phenomenon in one integral expression.

EFFECTIVE CONDUCTIVITY OF THE HETEROGENEOUS POLARIZABLE MEDIUM

In this section, we will derive a constructive approach for determining the effective conductivity of a heterogeneous polarizable medium. We have established above that to solve this problem, we have to find the average value of the material property tensor, $\langle \hat{\mathbf{m}} \rangle$. The last function can be found based on the integral representation 32.

Multiplying both sides of 32 by $\Delta\hat{\sigma}(\mathbf{r})$, we have

$$\hat{\mathbf{m}}(\mathbf{r}) \cdot \mathbf{E}^b = \Delta\hat{\sigma}(\mathbf{r}) \cdot \mathbf{E}^b + \Delta\hat{\sigma}(\mathbf{r}) \cdot \int\int\int_V \hat{\mathbf{G}}_b(\mathbf{r}/\mathbf{r}') \cdot \hat{\mathbf{q}}(\mathbf{r}')dv' \cdot \mathbf{E}^b. \quad (33)$$

Our goal is to find the material property tensor $\hat{\mathbf{m}}$. According to equation 30, this tensor is related to the volume-polarizability tensor $\hat{\mathbf{q}}$ by the following equation:

$$\hat{\mathbf{m}} = [\hat{\mathbf{I}} + \hat{\mathbf{p}}]^{-1}\hat{\mathbf{q}}. \quad (34)$$

Therefore, to find $\hat{\mathbf{m}}$, we need to determine tensor $\hat{\mathbf{q}}$ first. The solution of this problem is provided in Appendix C. According to that appendix, we have the following expression for the volume-polarizability tensor $\hat{\mathbf{q}}$:

$$\hat{\mathbf{q}}_l = [\hat{\mathbf{I}} - \Delta\hat{\sigma}_l^p \cdot \hat{\mathbf{\Gamma}}_l]^{-1} \cdot \Delta\hat{\sigma}_l^p \cdot [\hat{\mathbf{I}} - \hat{\mathbf{\Gamma}}_l \cdot \langle \hat{\mathbf{q}} \rangle], \quad (35)$$

where the average value of $\hat{\mathbf{q}}$ is given by the equation

$$\langle \hat{\mathbf{q}} \rangle = \langle [\hat{\mathbf{I}} - \Delta\hat{\sigma}^p \cdot \hat{\mathbf{\Gamma}}]^{-1} \rangle^{-1} \langle [\hat{\mathbf{I}} - \Delta\hat{\sigma}^p \cdot \hat{\mathbf{\Gamma}}]^{-1} \cdot \Delta\hat{\sigma}^p \rangle. \quad (36)$$

According to equation 30, the average value of the material-property tensor is

$$\langle \hat{\mathbf{m}} \rangle = \langle [\hat{\mathbf{I}} + \hat{\mathbf{p}}]^{-1}\hat{\mathbf{q}} \rangle. \quad (37)$$

Substituting equation 37 into equation 9, we finally have

$$\hat{\sigma}_e = \hat{\sigma}_b + \langle [\hat{\mathbf{I}} + \hat{\mathbf{p}}]^{-1}\hat{\mathbf{q}} \rangle = \hat{\sigma}_b + [\hat{\mathbf{I}} + \hat{\mathbf{p}}_0]^{-1}\hat{\mathbf{q}}_0 f_0 + \sum_{l=1}^{N} [\hat{\mathbf{I}} + \hat{\mathbf{p}}_l]^{-1}\hat{\mathbf{q}}_l f_l. \quad (38)$$

Equation 38 allows us to calculate the effective conductivity for any multiphase, polarized composite medium. This equation can be treated as an IP analog of the "average-t-matrix approximation" (ATA) of the theory of electronic propagation in disordered binary alloys (Soven, 1967).

SELF-CONSISTENT APPROXIMATION FOR EFFECTIVE CONDUCTIVITY

Note that the simplest choice for the average value of the volume-polarizability tensor $\langle \hat{\mathbf{q}} \rangle$ is

$$\langle \hat{\mathbf{q}} \rangle = 0, \quad (39)$$

because in this case, from Appendix C, equation C-10, we have

$$\hat{\mathbf{q}}_l = [\hat{\mathbf{I}} - \Delta\hat{\sigma}_l^p \cdot \hat{\mathbf{\Gamma}}_l]^{-1} \cdot \Delta\hat{\sigma}_l^p, \quad (40)$$

and

$$\langle \hat{\mathbf{q}} \rangle = \langle [\hat{\mathbf{I}} - \Delta\hat{\sigma}^p \cdot \hat{\mathbf{\Gamma}}]^{-1} \cdot \Delta\hat{\sigma}^p \rangle = [\hat{\mathbf{I}} - \Delta\hat{\sigma}_0^P \cdot \hat{\mathbf{\Gamma}}_0]^{-1} f_0 + \sum_{l=1}^{N} [\hat{\mathbf{I}} - \Delta\hat{\sigma}_l^p \cdot \hat{\mathbf{\Gamma}}_l]^{-1} f_l = 0. \quad (41)$$

Equation 41 can be treated as a loose IP analog of the self-consistency condition of the classical theory (EMT) presented in Stroud (1975). Detailed analysis shows that for a composite medium without any IP effect, equation 41 leads to the Bruggeman method of effective-conductivity determination (Bruggeman, 1935; Choi, 1999).

Substituting equation 40 into equation 34, we find

$$\hat{\mathbf{m}}_l = [\hat{\mathbf{I}} + \hat{\mathbf{p}}_l]^{-1}[\hat{\mathbf{I}} - \Delta\hat{\sigma}_l^p \cdot \hat{\mathbf{\Gamma}}_l]^{-1} \cdot [\hat{\mathbf{I}} + \hat{\mathbf{p}}_l] \cdot \Delta\hat{\sigma}_l. \quad (42)$$

In this case, expression 9 for the effective conductivity of the polarized inhomogeneous medium takes the form

$$\hat{\boldsymbol{\sigma}}_e = \hat{\boldsymbol{\sigma}}_b + [\hat{\mathbf{I}} + \hat{\mathbf{p}}_0]^{-1}[\hat{\mathbf{I}} - \Delta\hat{\boldsymbol{\sigma}}_0^p \cdot \hat{\mathbf{\Gamma}}_0]^{-1} \cdot [\hat{\mathbf{I}} + \hat{\mathbf{p}}_0] \cdot \Delta\hat{\boldsymbol{\sigma}}_0 f_0 + \sum_{l=1}^{N} [\hat{\mathbf{I}} + \hat{\mathbf{p}}_l]^{-1} \times [\hat{\mathbf{I}} - \Delta\hat{\boldsymbol{\sigma}}_l^P \cdot \hat{\mathbf{\Gamma}}_l]^{-1} \cdot [\hat{\mathbf{I}} + \hat{\mathbf{p}}_l] \cdot \Delta\hat{\boldsymbol{\sigma}}_l f_l.$$

In particular, if we select the background conductivity to be equal to the host medium conductivity,

$$\hat{\boldsymbol{\sigma}}_b = \hat{\boldsymbol{\sigma}}_0,$$

then

$$\hat{\boldsymbol{\sigma}}_e = \hat{\boldsymbol{\sigma}}_0 + \sum_{l=1}^{N} [\hat{\mathbf{I}} + \hat{\mathbf{p}}_l]^{-1}[\hat{\mathbf{I}} - \Delta\hat{\boldsymbol{\sigma}}_l^p \cdot \hat{\boldsymbol{\Gamma}}_l]^{-1} \cdot [\hat{\mathbf{I}} + \hat{\mathbf{p}}_l] \cdot \Delta\hat{\boldsymbol{\sigma}}_l f_l, \quad (43)$$

because $\Delta\hat{\boldsymbol{\sigma}}_0 = 0$.

Note that for heterogeneous media without polarizability, equation 43 corresponds to the Maxwell-Garnett theory of the composite geoelectric medium (Choi, 1999).

The last equation provides a general solution for the effective-conductivity problem for an arbitrary, multiphase, composite polarized medium. We will call the conductivity-relaxation model described by equation 43 a generalized effective-medium theory of the IP effect (GEMTIP) model.

EFFECTIVE RESISTIVITY OF THE ISOTROPIC MEDIUM FILLED WITH ISOTROPIC GRAINS OF ARBITRARY SHAPE: ANISOTROPY EFFECT

We consider first a composite model with isotropic grains of arbitrary shape. In this case, all conductivities become scalar functions:

$$\hat{\boldsymbol{\sigma}}_0 = \hat{\mathbf{I}}\sigma_0,\ \Delta\hat{\boldsymbol{\sigma}}_l = \hat{\mathbf{I}}\Delta\sigma_l,\ \Delta\hat{\boldsymbol{\sigma}}_l^p = (\hat{\mathbf{I}} + \hat{\mathbf{p}}_l)\Delta\sigma_l.$$

Therefore, we can write

$$\hat{\boldsymbol{\sigma}}_e = \hat{\mathbf{I}}\sigma_0 + \sum_{l=1}^{N} [\hat{\mathbf{I}} + \hat{\mathbf{p}}_l]^{-1}[\hat{\mathbf{I}} - (\hat{\mathbf{I}} + \hat{\mathbf{p}}_l)\Delta\sigma_l\hat{\boldsymbol{\Gamma}}_l]^{-1}[\hat{\mathbf{I}} + \hat{\mathbf{p}}_l]\Delta\sigma_l f_l, \quad (44)$$

where, according to the definition of the surface-polarizability tensor (see Table 1),

$$\hat{\mathbf{p}}_l = \xi_l\hat{\boldsymbol{\Gamma}}_l^{-1} \cdot \hat{\boldsymbol{\Lambda}}_l, \quad (45)$$

and ξ_l is equal to

$$\xi_l = k_l\sigma_0\sigma_l(\Delta\sigma_l)^{-1}. \quad (46)$$

It can be demonstrated that if the grains have nonisometric shape (e.g., ellipsoidal shape) but random orientation (see Figure 3), averaging of the tensor terms in expression 44 will result in scalarization. Therefore, the effective-medium conductivity will become a scalar function. However, if all the grains are oriented in one specific direction, as shown in Figure 4, the effective conductivity of this medium will become anisotropic.

Thus, the effective conductivity can be a tensor in spite of the fact that the background medium and all the grains are electrically isotropic. This tensorial property of the effective-medium conductivity provides a new insight into the anisotropy phenomenon in the IP effect. This effect is examined in full detail in Zhdanov et al. (2008).

FUNDAMENTAL IP MODEL: ISOTROPIC, MULTIPHASE HETEROGENEOUS MEDIUM FILLED WITH SPHERICAL INCLUSIONS

The GEMTIP model allows us to find the effective conductivity of a medium with inclusions that have arbitrary shape and electrical properties. That is why the new composite geoelectric model of the IP effect can be used to construct the effective conductivity for different realistic rock formations typical for mineralization zones and/or petroleum reservoirs.

In the present paper, however, as an illustration, I will present one fundamental IP model only: an isotropic, multiphase heterogeneous medium filled with spherical inclusions. This model, because of its relative simplicity, makes it possible to explain the close relationships between the new GEMTIP conductivity-relaxation model and an empirical Cole-Cole model (Cole and Cole, 1941) or a classical Wait's model (Wait, 1982).

Cole-Cole resistivity relaxation model

It was demonstrated in the pioneering work of Pelton (1977) that the Cole-Cole relaxation model can represent well the typical complex conductivity of polarized rock formations. In the framework of this model, the effective complex resistivity, $\rho_e(\omega)$, is described by the following well-known expression:

$$\rho_e(\omega) = \rho_0\left(1 - \eta\left(1 - \frac{1}{1 + (i\omega\tau)^C}\right)\right), \quad (47)$$

where ρ_0 is the DC resistivity (ohm-m), ω is the angular frequency (rad/sec), τ is the time parameter, η is the intrinsic chargeability (Seigel, 1959), and C is the relaxation parameter. The dimensionless intrinsic chargeability, η, characterizes the intensity of the IP effect.

Figure 5 presents examples of typical complex resistivity curves with the Cole-Cole model parameters defined according to Table 2.

One can see a significant difference among curves in this plot that correspond to Cole-Cole models with different parameters. Note also that the Cole-Cole curve gives only one possible example of the relaxation model. Several other models are discussed in the geophysical literature (e.g., see Kamenetsky, 1997). One of the important practical questions is the relationship between the Cole-Cole model parameters and the petrophysical characteristics of mineral-

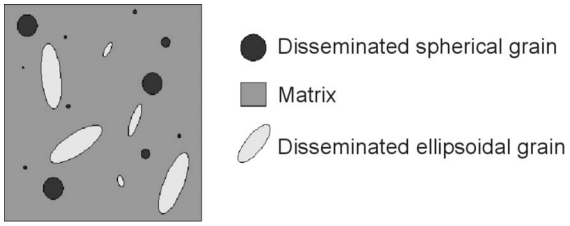

Figure 3. A typical example of a multiphase model of rock composed of a set of different types of randomly oriented grains.

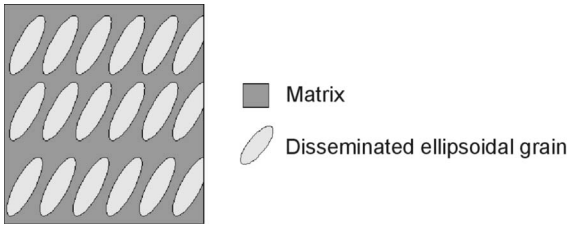

Figure 4. An example of electrically anisotropic media. A multiphase model of the rock is composed of a set of ellipsoidal grains oriented in one direction.

ized rocks. Several publications are dedicated specifically to the solution of this problem. However, most of the published results provide only a qualitative indication of the correlation between the Cole-Cole parameters and specific mineralization characteristics of the rocks, such as mineral grain sizes and physical properties.

Multiphase, composite polarized medium with spherical inclusions

In his pioneering work, Wait (1982) introduced a simplified model of the composite medium as a loading of spherical, conducting particles in a resistive background. The effective conductivity for this model was determined based on the equations of the static electric field. This model provided a foundation for the phenomenological theory of induced electrical polarization.

In the following sections, I will show that Wait's model appears as a special case of the GEMTIP model developed in this paper. I consider as an example an isotropic, multiphase composite model, with all model parameters described by the scalar functions. A composite model is formed by a homogeneous host medium of a volume V with a conductivity σ_0 filled with grains of spherical shape (Figure 6). We assume also that we have a set of N types of grains, with the lth grain type having radius a_l, conductivity σ_l, and surface-polarizability k_l. In this model, both the volume and the surface-depolarization tensors are constant scalar tensors (see Appendix B) equal to

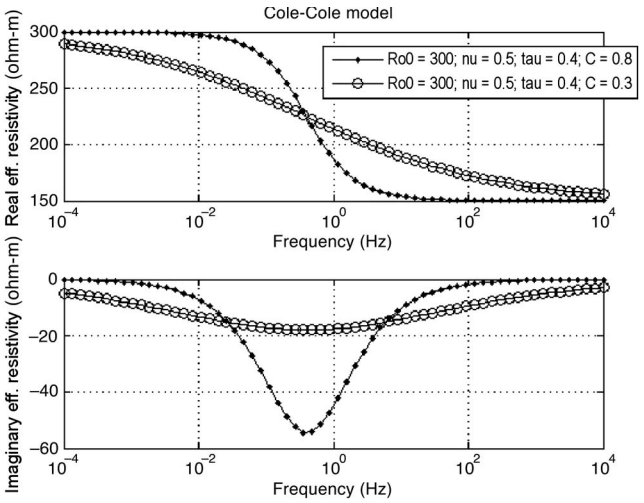

Figure 5. A typical example of a multiphase model of rock composed of a set of different types of randomly oriented grains. Examples of typical complex resistivity curves with the Cole-Cole model parameters. The upper panel shows the real part of the complex resistivity, and the bottom panel presents the imaginary part of the complex resistivity. Solid lines with dots represent the Cole-Cole model 1, and lines with circles correspond to Cole-Cole model 2.

Table 2. Cole-Cole models.

Cole-Cole model 1	Cole-Cole model 2
$\rho_0 = 300$ ohm-m	$\rho_0 = 300$ ohm-m
$\eta_1 = 0.5$	$\eta_2 = 0.5$
$\tau_1 = 0.4$	$\tau_2 = 0.4$
$C_1 = 0.8$	$C_2 = 0.3$

$$\hat{\mathbf{\Gamma}}_l = \Gamma_l \hat{\mathbf{I}} = -\hat{\mathbf{I}}\frac{1}{3\sigma_b}\hat{\mathbf{I}}, \quad \hat{\mathbf{\Lambda}}_l = \Lambda_l \hat{\mathbf{I}} = -\frac{2}{3\sigma_b a_l}\hat{\mathbf{I}}. \tag{48}$$

The corresponding tensor formulas for conductivity tensors and tensors $\hat{\mathbf{m}}$ and $\hat{\mathbf{q}}$ can be substituted by the scalar equations. For example, in Appendix C, equation C-10 for $\hat{\mathbf{q}}$ takes the form

$$q_l = [1 - \Delta\sigma_l^p \Gamma_l]^{-1} \Delta\sigma_l^p [1 - \Gamma_l \langle q \rangle], \tag{49}$$

and equation 34 for $\hat{\mathbf{m}}$ becomes

$$\begin{aligned} m_l &= [1 + p_l]^{-1} q_l \\ &= [1 - (1 + p_l)\Delta\sigma_l \Gamma_l]^{-1} \Delta\sigma_l [1 - \Gamma_l \langle q \rangle], \end{aligned} \tag{50}$$

where, according to equations 29 and 20,

$$p_l = 2k_l a_l^{-1} \sigma_b \sigma_l (\Delta\sigma_l)^{-1}. \tag{51}$$

In Appendix C, formula C-11 for $\langle \hat{\mathbf{q}} \rangle$ is simplified as well:

$$\begin{aligned} \langle q \rangle = &\langle [1 - (1 + p_l)\Delta\sigma_l \Gamma_l]^{-1} \rangle^{-1} \\ &\times \langle [1 - (1 + p_l)\Delta\sigma_l \Gamma_l]^{-1} (1 + p_l)\Delta\sigma_l \Gamma_l \rangle. \end{aligned} \tag{52}$$

In the framework of the self-consistent theory, the effective conductivity will be given by a scalar form of expression 42:

$$m_l = [1 - (1 + p_l)\Delta\sigma_l \Gamma_l]^{-1} \Delta\sigma_l. \tag{53}$$

Substituting equation 53 into equation 9, we obtain the following scalar formula for the effective conductivity of the polarized, inhomogeneous medium:

$$\begin{aligned} \sigma_e &= \sigma_b + \langle [1 - (1 + p_l)\Delta\sigma_l \Gamma_l]^{-1} \Delta\sigma_l \rangle \\ &= \sigma_b + [1 - (1 + p_0)\Delta\sigma_0 \Gamma_0]^{-1} \Delta\sigma_0 f_0 \\ &\quad + \sum_{l=1}^{N} [1 - (1 + p_l)\Delta\sigma_l \Gamma_l]^{-1} \Delta\sigma_l f_l. \end{aligned} \tag{54}$$

In particular, assuming $\sigma_b = \sigma_0$ and, therefore, $\Delta\sigma_0 = 0$, we write

$$\sigma_e = \sigma_0 + \sum_{l=1}^{N} [1 - (1 + p_l)\Delta\sigma_l \Gamma_l]^{-1} \Delta\sigma_l f_l. \tag{55}$$

Substituting expression 48 for the volume-depolarization tensor and equation 53 for p_l, we finally find

$$\sigma_e = \sigma_0 \left\{ 1 + 3 \sum_{l=1}^{N} \left[f_l \frac{\sigma_l - \sigma_0}{2\sigma_0 + \sigma_l + 2k_l a_l^{-1} \sigma_0 \sigma_l} \right] \right\}.$$

Figure 6. Multiphase composite polarized medium with spherical inclusions.

Multiplying the numerator and denominator by $\rho_l\rho_0$ (where $\rho_0 = 1/\sigma_0$, $\rho_l = 1/\sigma_l$), we obtain an equivalent expression for the effective resistivity of the composite polarized medium:

$$\rho_e = \rho_0\left\{1 + 3\sum_{l=1}^{N}\left[f_l\frac{\rho_0 - \rho_l}{2\rho_l + \rho_0 + 2k_l a_l^{-1}}\right]\right\}^{-1}. \quad (56)$$

It is well known from the experimental data that the surface-polarizability factor is a complex function of frequency (e.g., Luo and Zhang, 1998). Following Wait (1982), we adopt the model

$$k_l = \alpha_l(i\omega)^{-C_l}, \quad (57)$$

which fits the experimental data, where α_l is some empirical surface-polarizability coefficient, measured in the units $[\alpha_l] = (\text{Ohm} \times \text{m}^2)/\text{sec}^{C_l}$, and C_l is the relaxation parameter of the lth grain. Note that the GEMTIP model allows different forms of the surface-polarizability factor. However, equation 57 is the most widely used in practice.

Substituting equation 57 into expression 56, after some algebra, we have

$$\rho_e = \rho_0\left\{1 + \sum_{l=1}^{N}\left[f_l M_l\left[1 - \frac{1}{1 + (i\omega\tau_l)^{C_l}}\right]\right]\right\}^{-1}, \quad (58)$$

where

$$M_l = 3\frac{\rho_0 - \rho_l}{2\rho_l + \rho_0}, \quad (59)$$

and the time parameter τ_l of the lth grain is equal to

$$\tau_l = \left[\frac{a_l}{2\alpha_l}(2\rho_l + \rho_0)\right]^{1/C_l}. \quad (60)$$

Formula 58 provides a general analytic expression for the effective conductivity of the multiphase heterogeneous polarized medium, typical for mineralization zones.

I will present below some typical GEMTIP resistivity-relaxation models for the three-phase composite polarized media. The model is formed by a homogeneous host rock with a resistivity ρ_0 filled with two types of spherical grains, simulating, e.g., pyrite and chalcopyrite inclusions. The resistivities of these grains are $\rho_1 = 0.2$ ohm-m and $\rho_2 = 0.004$ ohm-m, respectively. We consider two types of GEMTIP models. For model 1, we change the surface-polarizability coefficient α_2 of the second grain while keeping all other parameters of the model fixed. For model 2, we change the radius of the second grain, a_2, only. The parameters of the models are given in Table 3.

Figures 7 and 8 present the real and imaginary parts of the complex effective resistivity for GEMTIP models 1 and 2. We notice first that in the case of the multiphase model, the resistivity-relaxation curve becomes more complicated than the conventional Cole-Cole curve (Figure 5). The resistivity plots might have not only one but several minima. Changing the parameters of the models affects the shape of the curves and the location of the minima in the imaginary parts of the resistivity plots. Note that this result corresponds well to the pioneering work of Zonge (1972), who predicted a double-peak resistivity-curve shape consistent with his observations on rock measurements in the laboratory (MacInnes, 2007).

Two-phase composite, polarized medium with spherical inclusions

In the case of a two-phase composite model, we have a homogeneous host medium of a volume V with a (complex) resistivity ρ_0 and spherical inclusions with resistivity ρ_1. Formula 56 is simplified:

$$\rho_e = \rho_0\left\{1 + f_1 M_1\left[1 - \frac{1}{1 + (i\omega\tau_1)^{C_1}}\right]\right\}^{-1}. \quad (61)$$

After some algebra, we arrive at the conventional Cole-Cole formula for the effective resistivity:

Table 3. Three-phase GEMTIP models.

Variable	Units	GEMTIP model 1	GEMTIP model 2
ρ_0	ohm-m	300	300
f_1	%	15	15
f_2	%	15	15
C_1	—	0.8	0.8
C_2	—	0.6	0.6
ρ_1	ohm-m	0.2	0.2
ρ_2	ohm-m	0.004	0.004
a_1	mm	0.2	0.2
a_2	mm	0.2	0.1; 0.2; 0.4; 0.8
α_1	$(\text{ohm-m}^2)/\text{sec}^{C_l}$	2	2
α_2	$(\text{ohm-m}^2)/\text{sec}^{C_l}$	0.4; 0.04; 0.004	0.04

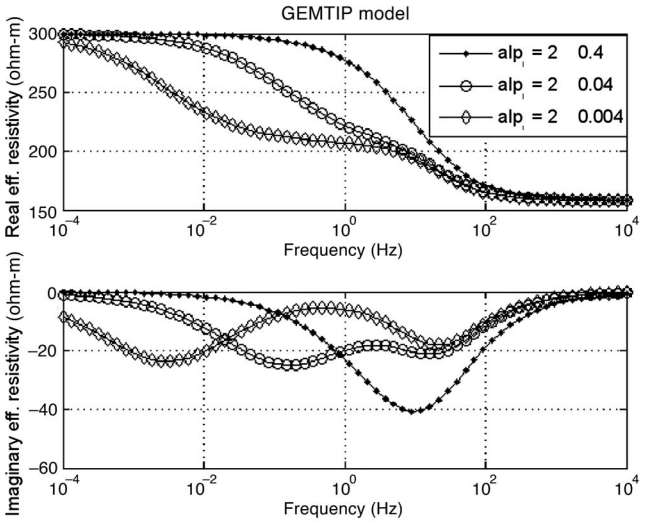

Figure 7. Resistivity-relaxation model of three-phase heterogeneous rock produced for GEMTIP model 1. The upper panel shows the real part of the complex-effective resistivity, and the bottom panel presents the imaginary part of the complex-effective resistivity. The three curves in each panel correspond to the different values of the surface-polarizability coefficient α_2 of the grain of the second type: $\alpha_2 = 0.4$, 0.04, and 0.004 $(\text{ohm-m}^2)/\text{sec}^{C_l}$, respectively.

$$\rho_e = \rho_0\left\{1 - \eta\left[1 - \frac{1}{1 + (i\omega\tau)^C}\right]\right\}, \qquad (62)$$

where

$$\eta = \frac{3f_1(\rho_0 - \rho_1)}{2\rho_1 + \rho_0 + 3f_1(\rho_0 - \rho_1)} \qquad (63)$$

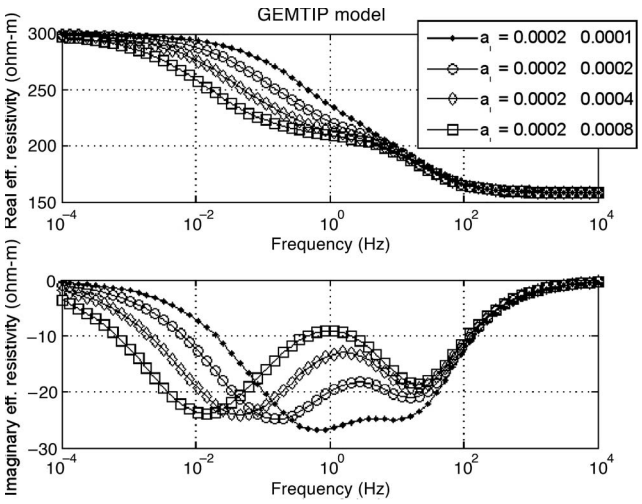

Figure 8. Resistivity-relaxation model of three-phase heterogeneous rock produced for GEMTIP model 2. The upper panel shows the real part of the complex effective resistivity, and the bottom panel presents the imaginary part of the complex effective resistivity. The four curves in each panel correspond to the different values of the radius a_2 of the grain of the second type: $a_2 = 0.1, 0.2, 0.4$, and 0.8 mm, respectively.

Table 4. GEMTIP resistivity-relaxation models of Ostrander and Zonge (1978) synthetic rocks.

Variable	Units	GEMTIP	Ostrander and Zonge
ρ_e	ohm-m		
ρ_0	ohm-m	300	300 ± 75
f_{pyrite}	%	15	—
$f_{\text{chalcopyrite}}$	%	15	—
C_{pyrite}	—	0.8	—
$C_{\text{chalcopyrite}}$	—	0.6	—
ρ_{pyrite}	ohm-m	0.2	0.2
$\rho_{\text{chalcopyrite}}$	ohm-m	0.004	0.004
a_{pyrite}	mm	0.2; 0.5; 0.7; 1;	0.2–0.5; 0.5–1; 1–2;
		1.2; 1.5; 2; 3	2–3
$a_{\text{chalcopyrite}}$	mm	0.2; 0.5; 0.7; 1;	0.2–0.5; 0.5–1; 1–2;
		1.2; 1.5; 2; 3	2–3
α_{pyrite}	$(\text{ohm-m}^2)/\text{sec}^{C_l}$	2	—
$\alpha_{\text{chalcopyrite}}$	$(\text{ohm-m}^2)/\text{sec}^{C_l}$	4	—

and

$$\tau = \left[\frac{a_1}{2\alpha_1}(2\rho_1 + \rho_0 + 3f_1(\rho_0 - \rho_1))\right]^{1/C}. \qquad (64)$$

Note that in equation 62, we use the same notations as in the original Cole-Cole formula 47.

Thus, both the conventional Cole-Cole model and the classical Wait's model appear as special cases of the general GEMTIP model of the complex resistivity of an isotropic, multiphase heterogeneous medium filled with spherical inclusions.

Comparison to Ostrander and Zonge data

The GEMTIP resistivity model of a multiphase, composite polarized medium with spherical inclusions was tested by a comparison with the published complex-resistivity data. Ostrander and Zonge (1978) studied synthetic rocks containing disseminated chalcopyrite and/or pyrite at specific grain sizes. They conducted complex-resistivity measurements for each synthetic rock and plotted the peak IP response frequency as a function of grain size for synthetic rocks containing either pyrite or chalcopyrite. As a result of the analysis of the experimental data, Ostrander and Zonge (1978) found a close correlation between the radius of sulfides and the frequency of the maximum IP response in the imaginary part of the complex-resistivity relaxation curve.

Emond et al. (2006) repeated the same experiment using the theoretical complex-resistivity model derived from the GEMTIP approach. Table 4 presents the GEMTIP variables used and the known parameters from Ostrander and Zonge (1978). The empirical parameters α and C are held constant for each mineral. These parameters were adjusted for each mineral until a good fit to the empirical data was established (Emond, 2007).

Figures 9 and 10 show the GEMTIP resistivity-relaxation models of Ostrander and Zonge for synthetic rocks containing pyrite. The lo-

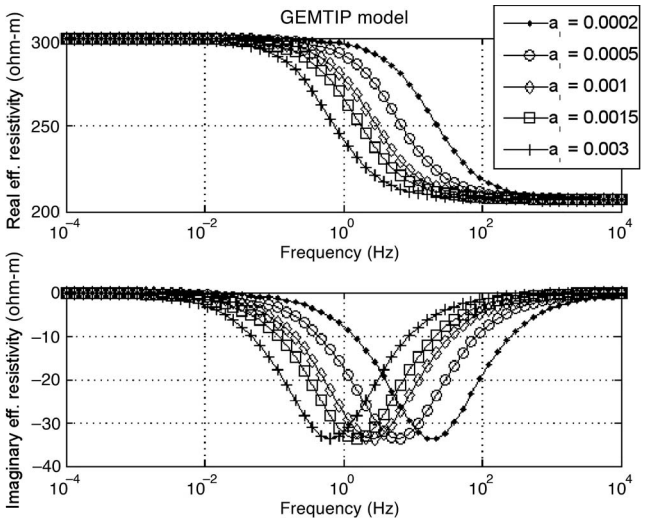

Figure 9. GEMTIP resistivity-relaxation models of Ostrander and Zonge (1978) for synthetic rocks containing pyrite. The upper panel shows the real part of the complex resistivity, and the bottom panel presents the imaginary part of the complex resistivity. The five curves in each panel correspond to the different values of the radius of the grain: $a_{\text{pyrite}} = 0.2, 0.5, 1, 1.5$, and 3 mm, respectively. The location of the minimum imaginary resistivity is the frequency of the maximum IP response.

cation of the peak imaginary resistivity is the frequency of maximum IP response (the minimum of the imaginary part of the complex effective resistivity). The GEMTIP-modeled data and the Ostrander and Zonge (1978) empirical data are plotted in Figure 11. The GEMTIP-modeled data yield the same trend of peak IP response frequency as the empirical results with respect to grain size.

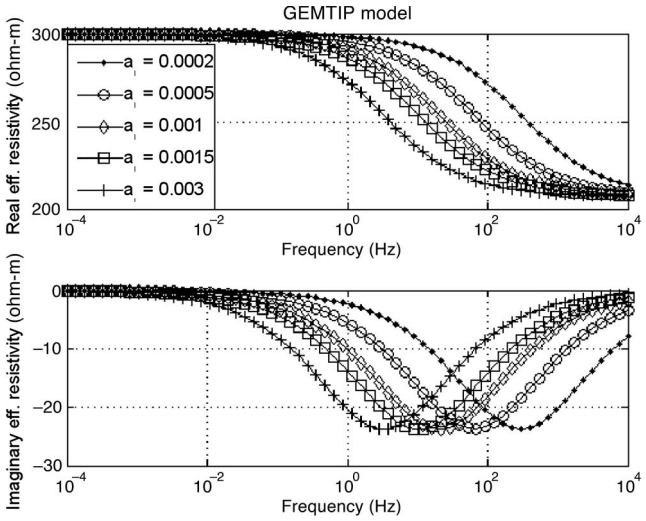

Figure 10. GEMTIP resistivity-relaxation models of Ostrander and Zonge (1978) for synthetic rocks containing chalcopyrite. The upper panel shows the real part of the complex resistivity, while the bottom panel presents the imaginary part of the complex resistivity. The five curves in each panel correspond to the different values of the radius of the grain: $a_{\text{chalcopyrite}} = 0.2$, 0.5, 1, 1.5, and 3 mm, respectively. The location of the minimum imaginary resistivity is the frequency of the maximum IP response.

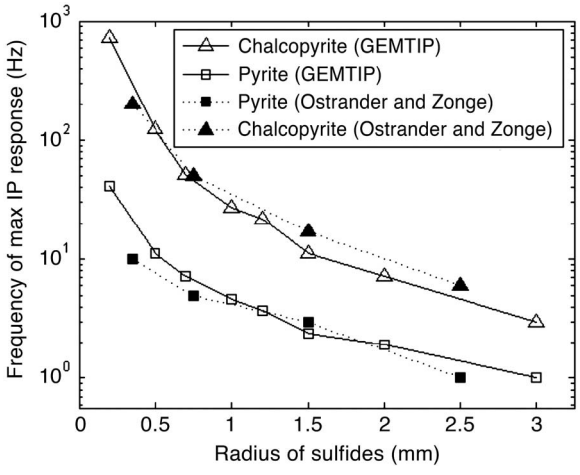

Figure 11. Comparison of GEMTIP-predicted data with empirical measurements of Ostrander and Zonge (1978) on synthetic rock samples. The good fit of the GEMTIP-modeled data with the empirical data indicates that GEMTIP can accurately model the trend in peak IP response as a function of grain size.

The exact volume fraction of chalcopyrite and pyrite used by Ostrander and Zonge (1978) for each sample is unknown. However, Figures 12 and 13 demonstrate that variations in volume fraction do not cause a large change in the peak IP frequency, indicating the comparison to be accurate as long as the volume fraction for each grain-size distribution sample is kept between 5% and 30% sulfides. Thus, I demonstrate that the GEMTIP approach can model well the IP effect of grain size on complex-effective resistivity.

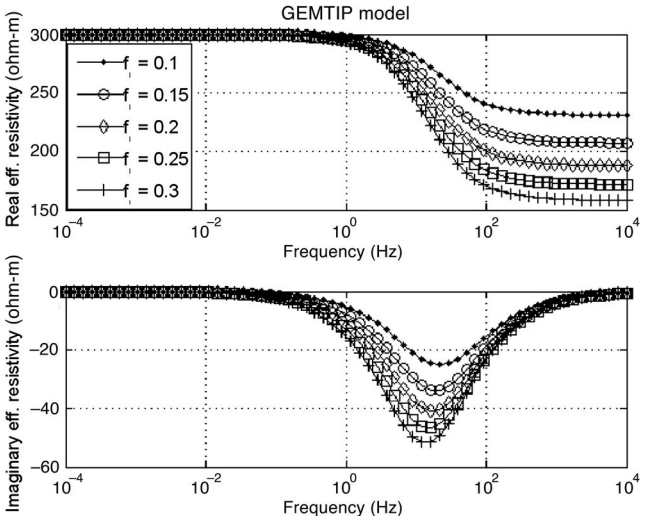

Figure 12. The small effect of volume fraction on maximum IP frequency shown in the graphed data is for 2-mm pyrite grains.

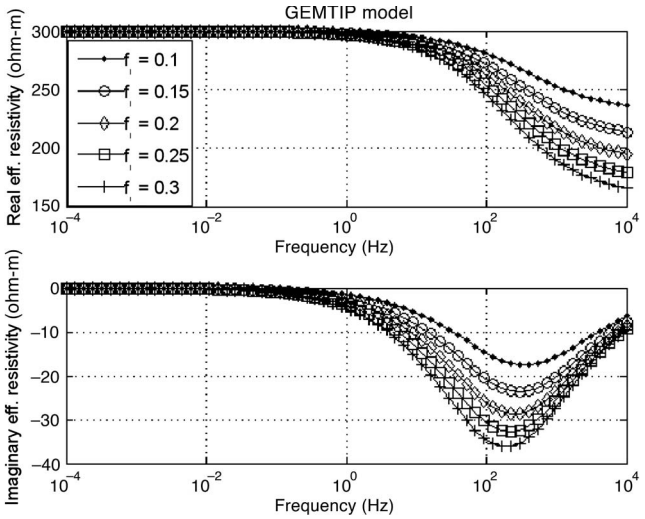

Figure 13. The small effect of volume fraction on maximum IP frequency shown in the graphed data is for 2-mm chalcopyrite grains.

CONCLUSIONS

I have developed an approach to constructing a physical-mathematical model of the IP effect that takes into account the true complexity of the rocks. This approach is based on the rock-physics description of the medium as a composite, heterogeneous multiphase formation. It takes into account both electromagnetic induction (EMI) and induced polarization (IP) effects related to the relaxation of polarized charges in rock formations.

The new generalized effective-medium theory of induced polarization (GEMTIP) provides a unified mathematical model of heterogeneity, multiphase structure, and polarizability of rocks. The GEMTIP model can be used for mineral-containing rocks and reservoir rocks. However, more research is needed to determine the practical limitations of the GEMTIP model. The geoelectric parameters of this model are determined by the intrinsic petrophysical and geometric characteristics of the composite medium: the mineralization and/or fluid content of the rocks and the matrix composition, porosity, anisotropy, and polarizability of the formations. Therefore, in principle, the effective complex conductivity of this new model can serve as a basis for determining the intrinsic characteristics of the polarizable rock formation from the observed electrical data, such as the volume content of the different minerals and/or the hydrocarbon saturation.

In this paper, I have illustrated the GEMTIP approach by a relatively simple model of the multiphase heterogeneous rocks with spherical inclusions that have different sizes and electrical properties. However, the general character of the GEMTIP model allows us to consider grains of arbitrary shape. Zhdanov et al. (2008) discuss a more complex model of heterogeneous rocks with ellipsoidal inclusions.

In summary, the GEMTIP approach expands the modeling capability of EM methods. This new method allows the spectral behavior of complex rock conductivity to be predicted based on its composition at the grain scale. Future research will be aimed at testing the new GEMTIP model with complex resistivity data and detailed mineralogical and petrophysical parameters of the rock samples.

ACKNOWLEDGMENTS

This work was supported by the National Energy Technology Laboratory of the U. S. Department of Energy under contract DE-FC26-04NT42081 and by the following members of the MDCA project: BHP Billiton World Exploration Inc., Kennecott Exploration Company, Placer Dome, Phelps Dodge Mining Company, and Zonge Engineering and Research Organization Inc. University of Utah master's student Abraham Emond has contributed to the numerical modeling of Ostrander and Zonge (1978) data. The author acknowledges the support of the University of Utah Consortium for Electromagnetic Modeling and Inversion (CEMI), which includes BAE Systems, Baker Atlas Logging Services, BGP China National Petroleum Corporation, BHP Billiton World Exploration Inc., BP, the Centre for Integrated Petroleum Research, EMGS, ENI S. p. A., ExxonMobil Upstream Research Company, Fugro, Halliburton Energy Services, INCO Exploration, Information Systems Laboratories, PGS, Newmont Mining Co., Norsk Hydro, OHM, Petrobras, Rio Tinto-Kennecott, Rocksource, Russian Research Center Kurchatov Institute, Schlumberger, Shell International Exploration and Production Inc., Statoil, Sumitomo Metal Mining Co., and Zonge Engineering and Research Organization.

APPENDIX A

EVOLUTION OF OUR METHOD AND ADDITIONAL BACKGROUND INFORMATION

This research was conducted at the University of Utah from 2004 through 2007 with support from the DOE and industry under the DOE program "Mining Industry of the Future: Exploration and Mining Technology." The project comprised a multipartner collaboration among the University of Utah, Kennecott Exploration Company, BHP Billiton World Exploration Inc., Placer Dome Inc., Phelps Dodge Mining Company, and Zonge Engineering and Research Organization. The major part of this research was funded by the National Energy Technology Laboratory of the U. S. Department of Energy under contract DE-FC26-04NT42081.

One of the main goals of this project was to develop a new theoretical model and a method for quantitative interpretation of IP data in a complex 3D environment. An important part of the research included the development of a new generalized effective-medium theory of the IP effect, which treated in a unified way different complex models of the multiphase composite models of the rocks.

I presented an original formulation of this generalized approach at the 76th Annual International Meeting of SEG in New Orleans (Zhdanov, 2006a). In addition, the basic ideas of using the Born-type QL approximation within the framework of GEMTIP were formulated in the patent application "Geophysical technique for mineral exploration and discrimination based on electromagnetic methods and associated systems," filed 22 July 2005, and granted U. S. Patent 7,324,899 on 29 January 2008. All these papers and patent documents are in the public domain and are freely available on the Internet (as well as the DOE report: Zhdanov, 2006b, New geophysical technique for mineral exploration and mineral discrimination based on electromagnetic methods, DE-FC26-04NT42081, Final report, available at http://www.osti.gov/bridge/servlets/purl/909271-Dykq2P/, accessed 22 December 2007).

Habashy and Abubakar (2007) employed the Born-type approximation within the framework of the EMT theory to derive a material-averaging formula similar to what was introduced originally in our papers on GEMTIP. Habashy and Abubakar do not include in their analysis the IP effect, however, which is the major subject of this paper. They point out that these new ideas could be useful in developing the effective numerical methods to study rock heterogeneity.

Indeed, an application of the GEMTIP theory and methods can make it practical to model the EM field in the complex heterogeneous rock formations by applying the effective-conductivity averaging method, developed within the framework of GEMTIP. This application of the GEMTIP method can constitute an important new area of EM research in the future.

APPENDIX B

CALCULATION OF THE DEPOLARIZATION TENSORS FOR A SPHERE

The generalized effective-medium theory of the induced polarization (GEMTIP), developed in this paper, requires the calculation of two depolarization tensors—the volume-depolarization tensor $\hat{\mathbf{\Gamma}}_0$ and the surface-depolarization tensor $\hat{\mathbf{\Lambda}}_0$ (see Table 1 for the definitions). The problem of the calculation of the volume-depolarization tensor for a sphere was discussed in many publications (e.g., see the

classic book by Landau and Lifshitz, 1984). However, we also need to compute the surface-depolarization tensor, $\hat{\mathbf{\Lambda}}_0$, which naturally appears in the GEMTIP model. The good news, however, is that the calculation of the surface-depolarization tensors can be reduced to the calculation of the conventional volume-depolarization tensor. That is why, for completeness, I begin this appendix with the calculation of the tensor $\hat{\mathbf{\Gamma}}_0$ for a sphere of a radius a:

$$\hat{\mathbf{\Gamma}}_0 = \nabla \int\int_{S_0} g_b(\mathbf{r}/\mathbf{r}')\mathbf{n}(\mathbf{r}')ds' = \frac{1}{4\pi\sigma_b}\int\int_{S_0}\frac{\mathbf{r}-\mathbf{r}'}{|\mathbf{r}-\mathbf{r}'|^3}\frac{\mathbf{r}'}{|\mathbf{r}'|}ds'.$$

In the center of the sphere $\mathbf{r} = \mathbf{0}$, we have

$$\hat{\mathbf{\Gamma}}_0 = -\frac{1}{4\pi\sigma_b a^2}\int\int_{S_0}\frac{\mathbf{r}'}{|\mathbf{r}'|}\frac{\mathbf{r}'}{|\mathbf{r}'|}ds' = -\frac{1}{4\pi\sigma_b a^2}\int\int_{S_0}\mathbf{n}(\mathbf{r}')\mathbf{n}(\mathbf{r}')ds', \qquad \text{(B-1)}$$

where $\mathbf{n}(\mathbf{r}')$ is a unit vector normal to the sphere

$$\mathbf{n}(\mathbf{r}') = \mathbf{r}'/|\mathbf{r}'| = \sum_{\gamma=x,y,z} n_\gamma \mathbf{d}_\gamma.$$

The integral of the diadic multiplication of the normal vectors $\mathbf{n}(\mathbf{r}')\mathbf{n}(\mathbf{r}')$ is equal to

$$\int\int_{S_0}\mathbf{n}(\mathbf{r}')\mathbf{n}(\mathbf{r}')ds' = \sum_{\alpha=x,y,z}\sum_{\beta=x,y,z}\int\int_{S_0} n_\alpha \mathbf{d}_\alpha n_\beta \mathbf{d}_\beta ds' = \int\int_{S_0}\frac{r_\alpha}{r}\frac{r_\beta}{r}ds\,\delta_{\alpha\beta} = \begin{cases} 0, & \alpha \neq \beta \\ \int\int_{S_0} n_\alpha n_\alpha ds = \frac{4\pi}{3}a^2 & \end{cases},$$

where $\delta_{\alpha\beta}$ is a symmetric Kronecker symbol.

Indeed, we have

$$\sum_{\alpha=x,y,z}\int\int_{S_0}\frac{r_\alpha}{r}\frac{r_\alpha}{r}ds = \int\int_{S_0}\frac{\Sigma_\alpha r_\alpha^2}{r^2}ds = \int\int_{S_0} ds = 4\pi a^2.$$

Therefore,

$$\int\int_{S_0} n_\alpha n_\alpha ds = \frac{4\pi}{3}a^2,$$

$$\int\int_{S_0} n_\alpha n_\beta ds = \frac{4\pi}{3}a^2\delta_{\alpha\beta},$$

and

$$\int\int_{S_0}\mathbf{n}(\mathbf{r}')\mathbf{n}(\mathbf{r}')ds' = \sum_\alpha\sum_\beta\frac{4\pi}{3}a^2\delta_{\alpha\beta}\mathbf{d}_\alpha\mathbf{d}_\beta = \frac{4\pi}{3}a^2\hat{\mathbf{I}}. \qquad \text{(B-2)}$$

Substituting expression B-2 into expression B-1, we have

$$\hat{\mathbf{\Gamma}}_0 = -\frac{1}{4\pi\sigma_b a^2}\int\int_{S_0}\mathbf{n}(\mathbf{r}')\mathbf{n}(\mathbf{r}')ds' = -\frac{1}{4\pi\sigma_b a^2}\frac{4\pi}{3}a^2\hat{\mathbf{I}} = -\frac{1}{3\sigma_b}\hat{\mathbf{I}}. \qquad \text{(B-3)}$$

In a similar way, using expression B-2, we can find the expression for a surface-depolarization tensor in the center of the sphere ($\mathbf{r} = \mathbf{0}$):

$$\hat{\mathbf{\Lambda}}_0 = \int\int_{S_0}\hat{\mathbf{G}}_b(\mathbf{r}/\mathbf{r}')\cdot\mathbf{n}(\mathbf{r}')\mathbf{n}(\mathbf{r}')ds' = \int\int_{S_0}\nabla\nabla' g_b(\mathbf{r}/\mathbf{r}')\cdot\mathbf{n}(\mathbf{r}')\mathbf{n}(\mathbf{r}')ds' = -\frac{2}{4\pi\sigma_b a^3}\int\int_{S_l}\frac{\mathbf{r}'}{|\mathbf{r}'|}\frac{\mathbf{r}'}{|\mathbf{r}'|}ds' = -\frac{2}{4\pi\sigma_b a^3}\int\int_{S_l}\mathbf{n}(\mathbf{r}')\mathbf{n}(\mathbf{r}')ds'. \qquad \text{(B-4)}$$

Substituting expression B-2 into expression B-4, we obtain

$$\hat{\mathbf{\Lambda}}_l = -\frac{2}{4\pi\sigma_b a^3}\frac{4\pi}{3}a^2\hat{\mathbf{I}} = -\frac{2}{3\sigma_b a_l}\hat{\mathbf{I}}. \qquad \text{(B-5)}$$

APPENDIX C

CALCULATION OF THE VOLUME-POLARIZABILITY TENSOR $\hat{\mathbf{Q}}$

In this appendix, I discuss the method of the calculation of the polarizability tensor $\hat{\mathbf{q}}$. One can obtain an integral equation for $\hat{\mathbf{q}}$ by multiplying both sides of equation 33 by $[\hat{\mathbf{I}} + \hat{\mathbf{p}}]$,

$$\hat{\mathbf{q}}(\mathbf{r}) = \Delta\hat{\sigma}^p(\mathbf{r}) + \Delta\hat{\sigma}^p(\mathbf{r})\cdot\int\int\int_V\hat{\mathbf{G}}_b(\mathbf{r}/\mathbf{r}')\cdot\hat{\mathbf{q}}(\mathbf{r}')dv', \qquad \text{(C-1)}$$

where $\Delta\hat{\sigma}^p(\mathbf{r})$ is a "polarized" anomalous conductivity

$$\Delta\hat{\sigma}^p(\mathbf{r}) = [\hat{\mathbf{I}} + \hat{\mathbf{p}}(\mathbf{r})]\cdot\Delta\hat{\sigma}(\mathbf{r}). \qquad \text{(C-2)}$$

The volume integral in equation C-1 can be represented as a sum of two integrals—over the volume of one grain, V_l, and over the remaining volume $(V - V_l)$:

$$\int\int\int_V \hat{\mathbf{G}}_b(\mathbf{r}/\mathbf{r}')\cdot\hat{\mathbf{q}}(\mathbf{r}')dv' = \int\int\int_{V-V_l} \hat{\mathbf{G}}_b(\mathbf{r}/\mathbf{r}')\cdot\hat{\mathbf{q}}(\mathbf{r}')dv' + \int\int\int_{V_l} \hat{\mathbf{G}}_b(\mathbf{r}/\mathbf{r}')\cdot\hat{\mathbf{q}}(\mathbf{r}')dv'. \quad \text{(C-3)}$$

We approximate the integral over $(V - V_l)$ by replacing $\hat{\mathbf{q}}(\mathbf{r}')$ by its average in V, and we calculate the integral over V_l, taking into account property 23: $\hat{\mathbf{q}}(\mathbf{r}') = \hat{\mathbf{q}}_l = \text{const}$. As a result, we obtain

$$\int\int\int_V \hat{\mathbf{G}}_b(\mathbf{r}/\mathbf{r}')\cdot\hat{\mathbf{q}}(\mathbf{r}')dv' \approx \int\int\int_{V-V_l} \hat{\mathbf{G}}_b(\mathbf{r}/\mathbf{r}')dv'\cdot\langle\hat{\mathbf{q}}\rangle + \int\int\int_{V_l} \hat{\mathbf{G}}_b(\mathbf{r}/\mathbf{r}')dv'\cdot\hat{\mathbf{q}}_l. \quad \text{(C-4)}$$

According to Gauss's theorem, the volume-depolarization tensor $\hat{\boldsymbol{\Gamma}}_l$ is equal to

$$\hat{\boldsymbol{\Gamma}}_l = \nabla\int\int\int_{V_l}\nabla' g_b(\mathbf{r}/\mathbf{r}')dv' = \nabla\int\int_{S_l} g_b(\mathbf{r}/\mathbf{r}')\mathbf{n}(\mathbf{r}')ds'. \quad \text{(C-5)}$$

We can calculate the external integral within the limits of the infinitely large volume V in a similar way, using Gauss's theorem for the external domain $(V - V_l)$:

$$\int\int\int_{V-V_l} \hat{\mathbf{G}}_b(\mathbf{r}/\mathbf{r}')dv' = -\hat{\boldsymbol{\Gamma}}_l. \quad \text{(C-6)}$$

Substituting equations C-5 and C-6 into C-4, we have

$$\int\int\int_V \hat{\mathbf{G}}_b(\mathbf{r}/\mathbf{r}')\cdot\hat{\mathbf{q}}(\mathbf{r}')dv' \approx -\hat{\boldsymbol{\Gamma}}_l\cdot\langle\hat{\mathbf{q}}\rangle + \hat{\boldsymbol{\Gamma}}_l\cdot\hat{\mathbf{q}}_l. \quad \text{(C-7)}$$

The last result reduces equation C-1 to

$$\hat{\mathbf{q}}(\mathbf{r}) = \Delta\hat{\sigma}^p(\mathbf{r}) + \Delta\hat{\sigma}^p(\mathbf{r})\cdot\hat{\boldsymbol{\Gamma}}_l\cdot[\hat{\mathbf{q}}_l - \langle\hat{\mathbf{q}}\rangle]. \quad \text{(C-8)}$$

Assuming in the last formula that $\mathbf{r}\in V_l$, we find

$$\hat{\mathbf{q}}_l = \Delta\hat{\sigma}^p_l + \Delta\hat{\sigma}^p_l\cdot\hat{\boldsymbol{\Gamma}}_l\cdot[\hat{\mathbf{q}}_l - \langle\hat{\mathbf{q}}\rangle]. \quad \text{(C-9)}$$

Solving equation C-9, we determine the volume-polarizability tensor, $\hat{\mathbf{q}}_l$, for every grain:

$$\hat{\mathbf{q}}_l = [\hat{\mathbf{I}} - \Delta\hat{\sigma}^p_l\cdot\hat{\boldsymbol{\Gamma}}_l]^{-1}\cdot\Delta\hat{\sigma}^p_l\cdot[\hat{\mathbf{I}} - \hat{\boldsymbol{\Gamma}}_l\cdot\langle\hat{\mathbf{q}}\rangle]. \quad \text{(C-10)}$$

Taking an average value of both sides of equation C-10 and solving the resulting equation for $\langle\hat{\mathbf{q}}\rangle$, we find

$$\langle\hat{\mathbf{q}}\rangle = \langle[\hat{\mathbf{I}} - \Delta\hat{\boldsymbol{\sigma}}^p\cdot\hat{\boldsymbol{\Gamma}}]^{-1}\rangle^{-1}\langle[\hat{\mathbf{I}} - \Delta\hat{\boldsymbol{\sigma}}^p\cdot\hat{\boldsymbol{\Gamma}}]^{-1}\cdot\Delta\hat{\boldsymbol{\sigma}}^p\rangle. \quad \text{(C-11)}$$

This completes the calculation of the volume-polarizability tensor $\hat{\mathbf{q}}$.

REFERENCES

Abubakar, A., and T. M. Habashy, 2005, A Green function formulation of the extended Born approximation for three-dimensional electromagnetic modeling: Wave Motion, **41**, 211–227.

Berryman, J. G., 2006, Effective medium theories for multicomponent poroelastic composites: Journal of Engineering Mechanics, **132**, 519–531.

Bockrih, J., and A. K. N. Reddy, 1973, Modern electrochemistry: v. 1 and 2: Plenum Press.

Bruggeman, D. A., 1935, Effective medium model for the optical properties of composite material: Annalen der Physik, Series 5, **24**, 636–664.

Choi, T. C., 1999, Effective medium theory, principles and applications: Oxford Science Publications.

Cole, K. S., and R. H. Cole, 1941, Dispersion and absorption in dielectrics: Journal of Chemistry and Physics, **9**, 343–351.

Davydycheva, S., N. Rykhlinsky, and P. Legeido, 2004, An electrical prospecting method for oil search using induced polarization effect: 74th Annual International Meeting, SEG, Expanded Abstracts, 604–607.

Dukhin, S. S., 1971, Dielectric properties of disperse systems, *in* E. Matijevic, ed., Surface and colloid science, v. 3: Wiley, 83–166.

Emond, A. M., 2007, Electromagnetic modeling of porphyry systems from the grain-scale to the deposit-scale using the generalized effective medium theory of induced polarization: M.S. thesis, University of Utah.

Emond, A., M. S. Zhdanov, and E. U. Petersen, 2006, Electromagnetic modeling based on the rock physics description of the true complexity of rocks: Applications to porphyry copper deposits: 76th Annual International Meeting, SEG, Expanded Abstracts, 1313–1317a.

Habashy, T. M., and A. Abubakar, 2007, A generalized material averaging formulation for modeling electromagnetic fields: Journal of Electromagnetic Waves and Applications, **21**, 1145–1159.

Kamenetsky, F. M., 1997, Transient geo-electromagnetics: GEOS.

Kazatchenko, E., M. Markov, and A. Mousatov, 2004, Joint inversion of acoustic and resistivity data for carbonate microstructure evaluation: Petrophysics, **45**, 130–140.

Klein, J. D., T. Biegler, and M. D. Hornet, 1984, Mineral interfacial processes in the method of induced polarization: Geophysics, **49**, 1105–1114.

Komarov, V. A., 1980, Electrical prospecting by induced polarization method: Nedra.

Kolundzija, B. M., and A. R. Djordjevic, 2002, Electromagnetic modeling of composite metallic and dielectric structures: Artech House.

Landau, L. D., and E. M. Lifshitz, 1984, Electrodynamics of the continuous medium, 2nd ed.: Elsevier Butterworse-Heinemann.

Landauer, R., 1978, Electrical conductivity in inhomogeneous media: AIP Conference Proceedings, **40**, 2–45.

Luo, Y., and G. Zhang, 1998, Theory and application of spectral induced polarization: SEG.

Marshall, D. J., and T. R. Madden, 1959, Induced polarization, a study of its causes: Geophysics, **24**, 790–816.

MacInnes, S., 2007, Complex resistivity modeling: Presented at the IP Symposium at the 77th Annual International Meeting, SEG.

Mendelson, K. S., and M. N. Cohen, 1982, The effect of grain anisotropy on the electrical properties of isotropic sedimentary rocks: Geophysics, **47**, 257–263.

Nelson, P. H., 1997, Induced polarization research at Kennecott, 1965–1977: The Leading Edge, **16**, 29–33.

Norris, A. N., P. Sheng, and A. J. Callegari, 1985, Effective medium theories for two-phase dielectric media: Applied Physics Letters, **57**, 1990–1996.

Oldenburg, D., and Y. Li, 1994, Inversion of induced polarization data: Geophysics, **59**, 1327–1341.

Ostrander, A. G., and K. L. Zonge, 1978, Complex resistivity measurements of sulfide-bearing synthetic rocks: 48th Annual International Meeting, SEG, Abstract M-6, 113.

Pelton, W. H., 1977, Interpretation of induced polarization and resistivity data: Ph.D. thesis, University of Utah.

Pelton, W. H., S. H. Ward, P. G. Hallof, W. R. Sill, and P. H. Nelson, 1978, Mineral discrimination and removal of inductive coupling with multifrequency IP: Geophysics, **43**, 588–609.

Seigel, H. O., 1959, Mathematical formulation and type curves for induced polarization: Geophysics, **24**, 547–565.

Seigel, H. O., M. Nabighian, D. F. Parasnis, and K. Vozoff, 2007, The early history of the induced polarization method: The Leading Edge, **26**, 312–321.

Sen, P., C. Scala, and M. H. Cohen, 1981, A self-similar model for sedimentary rocks with application to the dielectric constant of fused glass beads: Geophysics, **46**, 781–796.
Sheinman, S. M., 1969, Contemporary physical foundations of the electrical prospecting theory: Nedra.
Sheng, P., 1991, Consistent modeling of the electrical and elastic properties of sedimentary rocks: Geophysics, **56**, 1236–1243.
Shuev, R. T., and M. Johnson, 1973, On the phenomenology of electrical relaxation in rocks: Geophysics, **38**, 37–48.
Shwartz, L. M., 1994, Effective medium theory of electrical condition in two-component anisotropic composites: Physica A, **207**, 131–136.
Sihvola, A., 2000, Electromagnetic mixing formulae and applications, *in* P. J. B. Clarricoats, and E. V. Jull, eds., IEEE Electromagnetic Waves Series No. 47.
Soven, P., 1967, Coherent-potential model of substitutional disordered alloys: Physical Review, **156**, 809–813.
Stroud, D., 1975, Generalized effective medium approach to the conductivity of an inhomogeneous material: Physical Review B, **12**, 3368–3373.
Toumelin, E., and C. Torres-Verdín, 2007, 2D pore-scale simulation of wideband electromagnetic dispersion of saturated rocks: Geophysics, **72**, no. 3, F97–F110.
Vinegar, H. J., and M. H. Waxman, 1988, Induced polarization method and apparatus for distinguishing dispersed and laminated clay in earth formations: U. S. Patent 4769606.
Wait, J. R., 1959, The variable-frequency method, *in* J. R. Wait, ed., Overvoltage research and geophysical applications: Pergamon.
———, 1982, Geo-electromagnetism: Academic Press.
Wong, J., 1979, An electrochemical model of the induced-polarization phenomenon in disseminated sulfide ores: Geophysics, **44**, 1245–1265.
Wong, J., and D. W. Strangway, 1981, Induced polarization in disseminated rocks containing elongated mineralization sulfide ores: Geophysics, **46**, 1258–1268.
Yuval, and D. W. Oldenburg, 1997, Computation of Cole-Cole parameters from IP data: Geophysics, **62**, 436–448.
Zhdanov, M. S., 1988, Integral transforms in geophysics: Springer-Verlag.
———, 2002, Geophysical inverse theory and regularization problems: Elsevier.
———, 2006a, Generalized effective-medium theory of induced polarization: 76th Annual International Meeting, SEG, Expanded Abstracts, 805–809.
———, 2006b, New geophysical technique for mineral exploration and mineral discrimination based on electromagnetic methods, DE-FC26-04NT42081, Final report, http://www.osti.gov/bridge/servlets/purl/909271-Dykq2P/, accessed 22 December 2007.
———, 2008, Geophysical technique for mineral exploration and discrimination based on electromagnetic methods and associated systems: U. S. Patent 7,324,899 B2.
Zhdanov, M. S., V. I. Dmitriev, V. Burtman, A. Emond, and A. Gribenko, 2008, Anisotropy of induced polarization in the context of the generalized effective-medium theory: Proceedings of the Annual Meeting of the Consortium for Electromagnetic Modeling and Inversion, University of Utah, 61–94.
Zonge, K., 1972, Electrical properties of rocks as applied to geophysical prospecting: Ph.D. thesis, University of Arizona.
———, 1983, Case histories of an electromagnetic method for petroleum exploration: Proprietary data sale, Zonge Engineering and Research Organization, Inc.
Zonge, K., and J. C. Wynn, 1975, Recent advances and applications in complex resistivity measurements: Geophysics, **40**, 851–864.